The influence of the crystal lattice on coarsening in unstable epitaxial growth

M. Ahr[1]*, M. Biehl[1], M. Kinne[2], and W. Kinzel[1]
[1] Institut für Theoretische Physik
Julius-Maximilians-Universität Würzburg
Am Hubland
D-97074 Würzburg, Germany
[2] Lehrstuhl für Physikalische Chemie II
Egerlandstr. 3
D-91058 Erlangen, Germany

February 1, 2008

Abstract

We report the results of computer simulations of epitaxial growth in the presence of a large Schwoebel barrier on different crystal surfaces: simple cubic(001), bcc(001), simple hexagonal(001) and hcp(001). We find, that mounds coarse by a step edge diffusion driven process, if adatoms can diffuse relatively far along step edges without being hindered by kink-edge diffusion barriers. This yields the scaling exponents $\alpha = 1$, $\beta = 1/3$. These exponents are independent of the symmetry of the crystal surface. The crystal lattice, however, has strong effects on the morphology of the mounds, which are by no means restricted to trivial symmetry effects: while we observe pyramidal shapes on the simple lattices, on bcc and hcp there are two fundamentally different classes of mounds, which are encompanied by characteristic diffusion currents: a metastable one with rounded corners, and an actively coarsening configuration, which breaks the symmetry given by the crystal surface.

1 Introduction

In spite of considerable efforts [1-7], see [8] for an overview, a thorough theoretical understanding of the late phases of epitaxial crystal growth is still lacking. In this publication we investigate the problem of growth in the presence of a strong Schwoebel barrier, which hinders interlayer transport and leads to an instability of the flat surface. During an initial transient, *mounds* form on the surface, which then start to merge. It is generally accepted, that in this asymptotic *coarsening* regime the statistical properties of the surface remain invariant under a simultaneous transformation of spatial extension $\vec{x}$, height $h(\vec{x})$ and time t:

$$\vec{x} \to b\vec{x}; \quad h(\vec{x}) \to b^{\alpha} h; \quad t \to b^{z} t, \tag{1}$$

*e-mail: ahr@physik.uni-wuerzburg.de

where α and $\beta := \alpha/z$ are believed to be *universal* exponents, which do not depend on details of the model and b is an arbitrary factor. If the process of growth stabilizes a specific slope, this will yield $\alpha = 1$.

It was first pointed out by Siegert et. al. [3, 4], that lattice symmetries may play an important role in the coarsening process. These authors investigated continuum equations, using an analogy between coarsening and a phase ordering process, which has recently gained popularity [9]: areas of constant slope should correspond to domains of a constant order parameter. They derived scaling exponents $\alpha = 1, \beta = 1/3$ on surfaces with a triangular symmetry, and $\beta = 1/(3\sqrt{2})$ for generic cubic surfaces, while $\beta = 1/3$ requires a fine-tuning of parameters.

However, Monte-Carlo simulations [10, 11] have raised doubts on these predictions, since they yield $\beta \simeq 1/3$ on a simple cubic lattice for a great range of parameters. In this paper, we want to adress the following questions: (1) What are the *mesoscopic* processes which make the mounds coarse? (2) How does the coarsening process depend on the crystal lattice and its symmetries? (3) Do these results support a deeper analogy between coarsening and phase ordering?

2 The model

To answer these questions, we perform computer simulations of growth on (001)-surfaces of the simple cubic (sc) lattice, the simple hexagonal lattice (sh), the body-centered cubic (bcc) lattice and the hexagonal close packing (hcp). This is done under solid-on-solid conditions, i.e. the effects of overhangs or dislocations are being neglected. Then, the simple lattices can be represented by a square (sc) respectively a triangular mesh (sh) of integers, which denote the height $h(\vec{x})$ of the surface. We build the bcc (hcp) lattice out of two intersecting sc (sh) sublattices, which contain the even respectively odd heights[1]. Here, an adatom in a *stable* configuration is bound to 4 (3) neighbours below in the other sublattice, which will be denoted as *vertical neighbours* in the following. Particles with fewer vertical neighbours form overhangs, which are forbidden by the solid-on-solid condition. This is physically reasonable, since such particles are only weakly bound and therefore these configurations will be unstable. Additionally it may have neighbours in the *lateral* direction, which are in the same sublattice.

The investigation of the coarsening process requires a fast algorithm which allows for the simulation of the deposition of thick films on comparatively large systems. Standard kinetical Monte-Carlo techniques, which consider the moves of many particles on the surface simultaneously require computationally expensive bookkeeping procedures. This makes them too slow for our purpose. Instead, we simulate the moves of a *single* particle from deposition until an immobile state is reached [10, 11]:

An adatom impinges on a randomly chosen lattice site. Due to its momentum perpendicular to the surface, the particle may funnel downhill [12, 13, 14] to the lowest (vertical) neighbour site. On bcc and hcp this is repeated until it reaches a *stable site*, as defined above. On the simple lattices this is a site $\vec{x}$, where all nearest neighbour sites have a height $\geq h(\vec{x})$.

Then, the adatom diffuses on the surface. If the particle has no lateral neighbours, one of its neighbour sites is chosen at random. On the simple lattices, the particle moves to this site only if its height does not change, i.e. we introduce an infinite Schwoebel barrier. On the

[1]For simplicity, we assume the spacing between the layers to be 1 lattice constant. Our algorithm depends only on the *topology* of the lattice.

bcc or hcp lattice, the particle is moved to the neighbour site if it is stable. This condition implies an infinite Schwoebel barrier, too, since a transition into a different layer can proceed only via a weakly bound (unstable) transient state. This procedure is repeated until either a lateral neighbour is reached or l_d^2 steps have been performed. The simulation of single particles requires an effective representation of the collisions of diffusing adatoms, which form a stable nucleaus. The diffusion length l_d corresponds to the mean free path length and depends on the diffusion constant D and the particle flux F: $l_d \propto (D/F)^{1/6}$ [15].

As soon as a particle has a lateral neighbour, it is bound to it. This process is irreversible in the sense that we forbid diffusion processes which reduce the number of bonds, like the detachement from a step edge. However, the adatom may diffuse along the edge. After l_k^2 steps, or if the particle has reached a kink site, it is fixed to the surface. If not stated otherwise, diffusion around corners is allowed.

Within this model, we measure time t in units of the time needed to deposit a monolayer. This algorithm may be programmed very efficiently and is about an order of magnitude faster than full diffusion Monte-Carlo algorithms.

In all our simulations, we choose $l_d = 15$. The diffusion length sets the initial island distance only, while its influence can be neglected in the later phases of growth, when the typical terrace width is much smaller than l_d. We simulate a variety of different values of the step edge diffusion length l_k in the range between $l_k = 1$ and $l_k = 20$. The simulations are performed on a square of $N \times N$ lattice constants using periodic boundary conditions (bcc and sc), respectively a regular hexagon with edges of length M (hcp and sh) using helical boundary conditions, our standard values being $N = 512$ and $M = 300$. For every parameter set, we have performed 7 independent simulation runs.

3 Surface morphologies

During the first ≈ 100 monolayers of growth on an initially flat surface, islands nucleate, on which mounds build up and take on their stable slope. Then, the asymptotical coarsening regime starts. As expected, on the simple lattices the mounds obtain regular shapes, which are determined by the symmetry of the surface: square pyramids on sc, hexagonal ones on sh. On bcc and hcp however, *rounded* corners as well as sharp corners can be found (figures 1 b, 2). Here one finds two fundamentally different types of mounds: On the one hand, there are mounds, where *all* corners are rounded with octagonal shapes on bcc (figure 2a), and 12-cornered ones on hcp. On the other hand, one observes a *breaking* of the *symmetry* given by the lattice: approximately triangular mounds on hcp (figure 1 b) and oval shapes on bcc (figure 2b), where every second of the corners is sharp, while the others are rounded. We have observed, that in the process of coarsening, on all lattice structures mounds merge preferentially at the *corners*, while mounds touching at the flanks are a *metastable* configuration. On bcc and hcp, the metastable configuration is made of mounds with completely rounded corners. Mounds, whose shapes break the lattice symmetry, are always in the course of merging with a neighbour they touch with a sharp corner [16].

To characterize the morphology quantitatively, we investigate the slopes $\vec{m} = \nabla h$ of the surface. On average, $|\vec{m}|$ obtains a value which can be estimated by a simple argument [17]: The Schwoebel effect yields an uphill current due to the preferential attachement of particles on terraces from below, which is compensated by a downhill current due to funneling. If we assume, that a particle reaches its final height after at most one incorporation step, the sc and

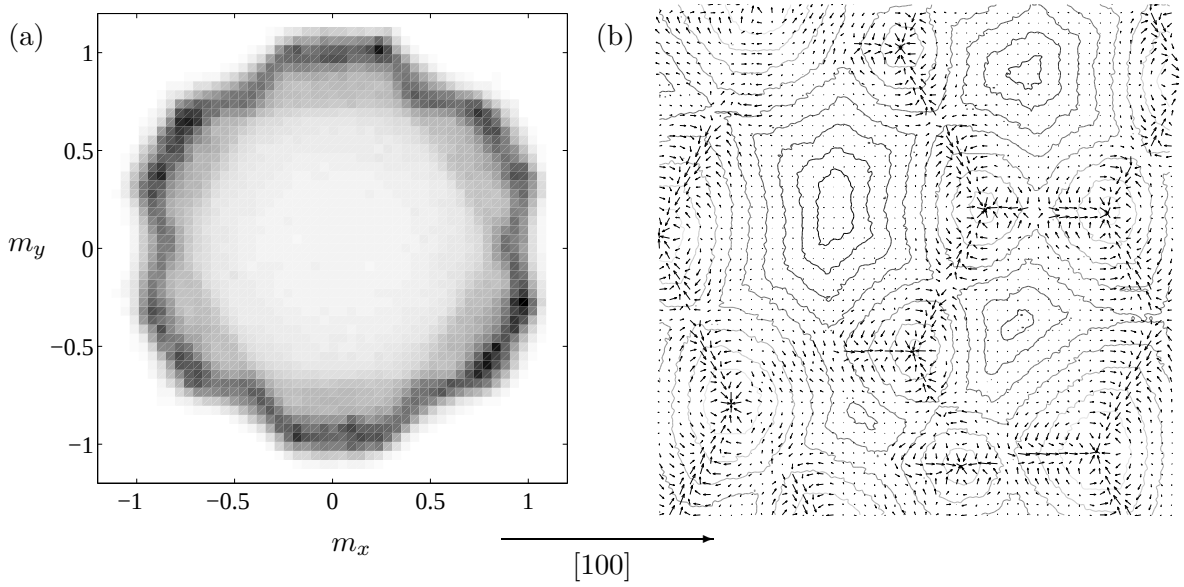

Figure 1: Simulation results on hcp ($M = 300$, $l_d = 15$, $l_k = 10$, $t = 20000$ML). Panel a: Histogram of slopes (density plot). High probabilities are drawn dark. Panel b: Contour plot of a part of size 250×250 lattice constants of the surface. High levels are plotted in light grey. The arrows show the surface current, as measured during deposition of additional 200ML.

the sh surface select $|\vec{m}| = 1/2$, while bcc and hcp select $|\vec{m}| = 1$. In practice, the selected slopes are slightly smaller, since the maximal number of incorporation steps in the funneling process is unlimited. Since a direct computation of the numerical gradient of simulated surfaces fails due to the discrete heights, we first apply a gaussian filter with variance $\sigma = 4$. This value has turned out to be a good compromise: it removes the atomistic structure, but preserves the shape of the mounds. Figure 1a shows a two-dimensional histogram of the slopes on hcp surfaces: due to the round shapes of the mounds, one finds a pronounced maximum of the probability density function in every direction of $\vec{m}$. The most probable value of $|\vec{m}|$ has a directional dependence: it is *minimal* in the lattice directions (0.88 ± 0.02), and *maximal* (0.99 ± 0.02) in the intermediary directions. Consequently, the rounded corners are *steeper* than the flanks. On bcc the results are equivalent, apart from the different symmetry, while they are rather trivial on sc and sh: a regular square respectively hexagon of slightly broadened peaks, which correspond to the flanks of the mounds.

4 Diffusion currents

To gain deeper insight into the coarsening process, we investigate the *material transport* on mesoscopic lengthscales, which can be done by tracing the motion of particles on the surface. On all lattice structures, we observe a strong uphill current at the corners of mounds, which is a geometrical effect: an adatom attaching at the corner is transported over a mean distance l_k, namely with equal probability along either of the two flanks of the mound. This results in a net current $\vec{j}$ in the direction of the bisector of the angle at the corner, which is directed

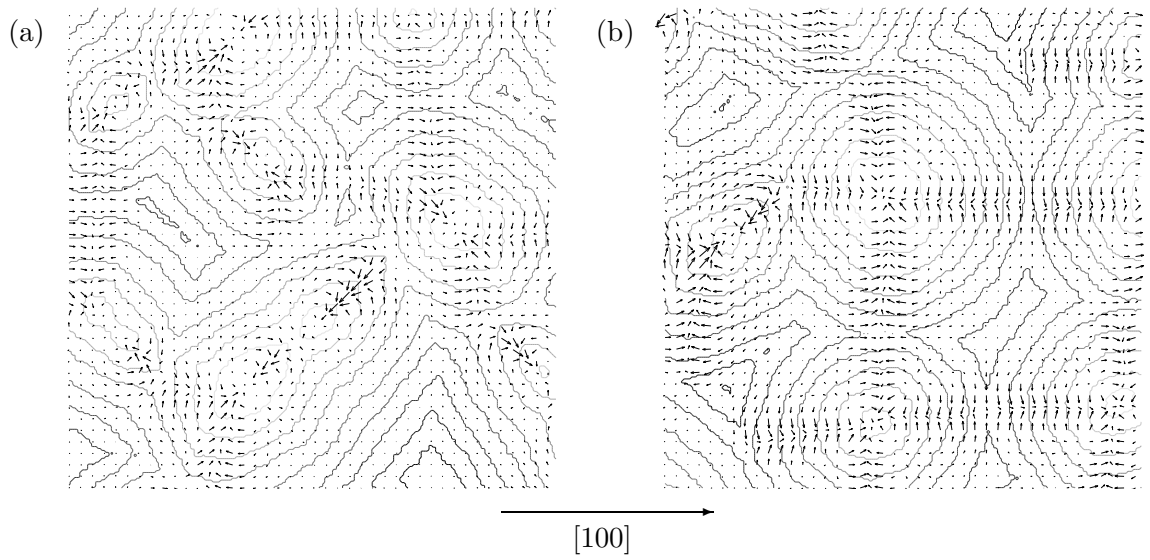

Figure 2: Contour plots of parts of size 250×250 lattice constants of bcc surfaces ($N = 512$, $l_d = 15$, $l_k = 10$, $t = 20000$ML). Panel a: section dominated by quickly coarsening mounds breaking the surface symmetry. Panel b: metastable configuration.

uphill. A simple calculation yields

$$|\vec{j}| = r_a l_k \cos\frac{\phi}{2}$$

if there is a straight step edge of length $\gg l_k$, which is the case on the simple lattices. Here r_a is the rate paricles attache at a step edge with, $\phi = \pi/2$ on surfaces with cubic symmetry and $\phi = 2\pi/3$ on hexagonal surfaces.

On the bcc and the hcp lattice however, material transport along step edges is severely restricted due to the rounded corners. There, particles diffusing along the step edge are on average *reflected*, which leads to a current towards the middle of the smooth step edges at the flanks of mounds in the metastable configuration, which have an extension $\approx l_k$ (figure 2b). This current has a non-vanishing *uphill* component due to the Schwoebel effect. On the rounded corners on the contrary, one observes a weak *downhill* current. This is explained by the observation of steep gradients (figure 1 a), at which the downhill current due to funneling dominates the uphill current of the Schwoebel effect. On these surfaces the stable slope, at which the currents cancel, is *not* assumed *locally*, but only in the *global* average, which results in spatial current patterns on the surface. An analogous behaviour is observed at the symmetry-breaking, merging mounds (figures 1b, 2a). Here, the smooth edges are in the proximity of the sharp corners. Particles are reflected at the rounded corners, too. This yields a net current towards the sharp corners, which *compensates* the geometrically induced uphill current exactly, if the smooth edges have a length l_k. This fact explains the broken symmetry of these mounds: if there is any process, which transports matter towards sharp corners, this material is not completely diffusing inward, as would be the case on pyramidal mounds, but is attached to the corner and makes it overgrow its neighbours. Merging of mounds, however,

is such a process: consider a terrace, which goes around two mounds touching each other at the corners. Due to its curvature, in this contact zone there is a high concentration of kink sites, which make it a *sink* for diffusing particles.

5 Theoretical estimation of scaling exponents

Our observation, that mounds merge perferentially in positions with touching corners, gives strong evidence that the current which fills the gap between two mounds, plays a dominant role in the process of coarsening, at least in the case of large l_k, where it is efficient. If this is the case, then a simple consideration yields the scaling exponents: Due to step edge diffusion, adatoms are transported over a typical distance l_k. If l_k is noticeably greater than a few lattice constants, this is much larger than the average terrace width. Then, material transport via diffusion on terraces is small compared to transport via step edge diffusion and can be neglected. Figure 1b shows, that the current into the gap is significant on a few atomic layers in the vicinity of the contact point only. In consequence, this current is *independent* of the size of the mounds, if the latter is much greater then l_k. Since the volume of the gap is proportional to L^3, if L is the typical distance between the mounds, it will take a time $t \sim L^3$ to fill it. In consequence, $L \sim t^{1/3} \Longrightarrow z = 3$. Since $\alpha = 1$ in the presence of slope selection, this yields $\beta = 1/3$. In contrast to the effects discussed in [3, 4] these considerations are completely independent of lattice symmetries. In [5, 6] a similar argument has been applied to the case of coarsening in the absence of dominant step edge diffusion processes ("bond energy driven coarsening"), where material is transported mainly by terrace diffusion. This yields $\beta = 1/4$. The same exponent is obtained, if coarsening is exclusively due to fluctuations in the particle beam ("noise assisted coarsening"). We expect, that these processes dominate step edge diffusion in the limit of small l_k, which leads to a transient from $\beta = 1/4$ to $\beta = 1/3$, when l_k is increased.

6 Measurement of scaling exponents

We apply a variety of methods to measure the scaling exponents. This is important as a consistency check and to eliminate systematical errors which might be intrinsical to some methods. First, β can be obtained from the increase of the *surface with* $w(t) = \left\langle \left(h(\vec{x},t) - \langle h \rangle (t)\right)^2 \right\rangle^{1/2}$ with time. Equation 1 corresponds to $w(t) \sim t^\beta$ [18]. This power law behaviour may be corrupted by the presence of noise on the surface profile, an aditional contribution to $w(t)$ which has been called *intrinsic width* [19]. Similarly, the *number of mounds* n_m in the system will decrease like $t^{-2/z}$, if this scaling hypothesis holds. We measure n_m by counting the number of *top terraces* in the system. Since a single particle is counted as a terrace, this method may be misleading, if particles nucleate on terraces at the flanks of mounds. A method which is widely used in the literature uses the fourier transform $\hat{h}(\vec{k})$[2]: The *structure factor* $S(\vec{k}) := \left\langle \hat{h}(\vec{k})\hat{h}(-\vec{k}) \right\rangle$ will be maximum at nonzero wavenumbers $|\vec{k}_m| = 2\pi/l_m$, if there are structures at a typical lengthscale l_m on the surface. Since $l_m \sim t^{1/z}$, $|\vec{k}_m|$ will decay $\sim t^{-1/z}$. In practice, a direct search for the maximum often fails due to noise effects; one avoids this problem by calculating the averages $k_m^{(p)} := \left\langle \left(\sum_{\vec{k}} |\vec{k}| S(\vec{k})^p\right) / \sum_{\vec{k}} S(\vec{k})^p \right\rangle$, however, the choice

[2]The mean surface height is subtracted before performing the fourier transform.

of the correct power p is a bit arbitrary.

6.1 The wavelet method

To avoid these difficulties, we propose a method which exploits the continuous wavelet transform

$$\vec{T}_{\vec{\Psi}}[h](\vec{b},a) := \frac{1}{a}\int d^2x \begin{pmatrix} \Psi_1((\vec{x}-\vec{b})/a) \\ \Psi_2((\vec{x}-\vec{b})/a) \end{pmatrix} h(\vec{x}) \tag{2}$$

of the surface heights. Here, the wavelets Ψ_1, Ψ_2 are defined as partial derivatives of a radially symmetrical filter $\Phi(\vec{x})$, which we choose to be a gaussian: $\Psi_1 := \partial\Phi/\partial x$, $\Psi_2 := \partial\Phi/\partial y$. The basic idea ot this transform is to convolve $h(\vec{x})$ with the wavelets, which are *dilated* with the scale a. This makes it a natural tool to search for the typical lengthscale a_t of structures on the surface. In [20, 21], it has been proposed to investigate the *wavelet transform modulus maxima* (WTMM). They are defined as local maxima of the *modulus* $M_{\vec{\Psi}}[h](\vec{b},a) := |\vec{T}_{\vec{\Psi}}[h](\vec{b},a)|$ in the direction of $\vec{T}_{\vec{\Psi}}$. The search for the WTMM is equivalent to *edge detection*: they lie on connected curves, which trace the contours of objects of size $\approx a$. We investigate the average of the WTMM on the scale a

$$W_m(a) := \left\langle M_{\vec{\Psi}}[h](\vec{b},a)\right\rangle_{\vec{b}=\mathrm{WTMM}}. \tag{3}$$

This function has a pronounced maximum at a value $a_m \propto a_t$, which is the scale that contains the most relevant contributions to the surface morphology. On mounded surfaces, $a_m \sim t^{1/z}$ is proportional to the *lateral size* of the mounds, while $W_m(a_m) \sim t^{\beta}$ is a measure for their heights. This procedure has several advantages compared to the standard methods used in the literature: (1) The detection of the WTMM leads to an efficient suppression of noise, and therefore eliminates the intrinsic width. (2) Since only the most important lengthscale is considered, the results may not be corrupted by details of the surface morphology on small lengthscales. (3) Appropriate wavelets are well localized both in real space and in fourier space. Therefore, this analysis combines the advantages of both real space techniques, like the counting on mounds, and fourier techniques, like the calculation of k_m^p. We have tested it both with artifical test surfaces and various toy models of growth and found a clear superiority to the standard methods, especially in the presence of noise, which should make it interesting for experimental investigations. Details will be given in a forthcoming publication.

6.2 Results

In our simulations, the asymptotic scaling behaviour is obtained after a long initial transient of ≈ 100 monolayers. Since after this transient only a comparatively small number of mounds is left on the surface, the measurement of exponents is complicated by finite size effects: due to the periodicity of the system, there is a *self-interaction* of the currents on the mounds, if their size is no more small compared to the system size. We measure $\alpha \approx 1$ for all $l_k > 1$, a consequence of slope selection. At $l_k = 1$ however, we measure smaller values, which *do* depend on the crystal lattice: $\alpha = 0.85$ on bcc and $\alpha = 0.94$ on hcp. A similar effect was observed in [10, 11] on the simple cubic lattice. We remark, that our results are independent of the method which was applied to measure the exponents. In figure 3, β is plotted as a function of l_k. Clearly, its value does *not* depend systematically on the *symmetry* of the crystal surface. We find no significant deviations between β on bcc and on hcp (sc and sh).

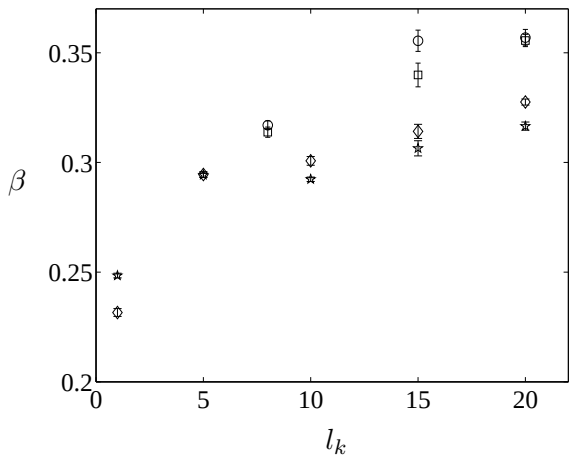

Figure 3: β, as obtained from the wavelet method, as a function of the step edge diffusion length. Diamonds: bcc lattice, squares: sc, stars: hcp, circles: sh. Results from measurements of β from the surface witdh are identical within the error bars. These have been estimated from the logarithmic fits; we expect the true errors to be larger due to systematical deviations.

As already observed in [10, 11], there is a dependence of β on the step edge diffusion length. One obtains values $\approx 1/4$ at $l_k = 1$ and higher values at greater l_k. The values obtained at large l_k are compatible with $\beta = 1/3$. As indicated above, we explain this transient as a competition between different coarsening mechanisms: At large l_k the merging of mounds should proceed mainly by the step edge diffusion driven transport of material into the gap, at small l_k it is dominated by noise assisted coarsening and/or bond energy driven coarsening. This competition might also explain, why the exponents measured on bcc and hcp are still slightly smaller than those obtained on the simple lattices even at values of l_k as large as 20, since the symmetry breaking of the mounds on these lattices halves the number of corners which are active in the coarsening process.

All the simulation results reported above have been obtained in simulations with unhindered step edge diffusion. To further corroborate our ideas of the coarsening process, we have also performed simulations with a corner diffusion barrier. A particle may diffuse at most l_k steps along a straight step edge, but diffusion around corners is forbidden. Then, we observe *no symmetry breaking* of the mounds, which now obtain regular polygonal shapes on all lattice structures. These are rotated by an angle of 45 degrees against the lattice directions on cubic surfaces and 30 degrees on hexagonal ones. Due to the absence of aligned step edges, material transport by step edge diffusion is severely restricted under these conditions. Thus, we measure only small diffusion currents, and observe no pronounced long-range order in the flux lines. Here, we find $\alpha \approx 1$, $\beta \approx 0.25$ on *all* lattices, *independent* of the step edge diffusion length. This slow coarsening in absence of the characteristic features of step edge diffusion driven coarsening - currents on mesoscopic lengthscales and symmetry breaking on bcc and hcp - strongly supports the important role of this mechanism for fast coarsening with $\beta = 1/3$.

7 Conclusions

In summary, we have presented a detailed investigation of the coarsening process in epitaxial growth. Our most important finding is, that the crystal lattice has a considerable influence on the morphology of the growing surface, which is by no means restricted to trivial symmetry effects. In spite of these differences, in the limit of large step edge diffusion lengths, the

mounds coarse according to power laws with universal exponents. We obtain $\beta \approx 1/3$ in the case of unhindered step edge diffusion and $\beta \approx 1/4$ in the case of restricted step edge diffusion.

These results contradict previous studies of the coarsening process using continuum equations [2, 3, 4], which predict slower coarsening on surfaces with a cubic symmetry. In these publications, equations have been studied, which are invariant under the transformation $h(\vec{x}) \rightarrow -h(\vec{x})$. This symmetry reflects itself also in the up-down-symmetry of the solutions of these equations. Clearly, our simulation results *break* this symmetry. In figures 1a, 2 the contours of the mounds and those of the valleys are clearly distinct. This is also true for the *currents*, especially the step edge diffusion current, which dominates the coarsening behaviour in the limit of large l_k and unhindered step edge diffusion and determines the scaling exponents. Since the symmetrical equations do not only fail to describe the morphology of the surface correctly, but also predict the wrong universality classes, we conclude, that the breaking of the up-down symmetry is a central feature of unstable epitaxial growth.

However, we find it difficult to interpret this result in the context of an analogy to a phase ordering process, where the local slope of the surface corresponds to an order parameter. In this picture, the importance of the breaking of up-down symmetry leads to the conclusion, that now the stability of a domain wall between areas of constant slope is a complicated function of both the *orientation* of the wall and the *order paramters* on both sides of it. Additionally, in contrast to the simple lattices, where there are only 4 (sc) respectively 6 (sh) stable slopes, on bcc and hcp one would have to deal with an order parameter, which obtains *continuous* values.

In any case, the behaviour of our models, which implement the microscopic processes on the surface, is governed by rules, which are much more complex than those implemented in all the continuum models we know. Differences are by no means restricted to some details, but have a fundamental influence on the behaviour of the system on large lengthscales.

References

[1] M. Kalff, P. Smilauer, G. Comsa, T. Michely, Surface Science **426**, L447, 1999

[2] M. Rost, J. Krug, Phys. Rev. E **55** (4), 3952, 1997

[3] M. Siegert, M. Plischke, R. K. P. Zia, Phys. Rev. Lett. **78** (19), 3705, 1997

[4] M. Siegert, Phys. Rev. Lett. **81** (25), 5481, 1998

[5] L.-H. Tang, P. Smilauer, D. D. Vvedensky, Eur. J. Phys. B **2**, 409, 1998

[6] L.-H. Tang, Physica A **254**, 135, 1998

[7] D. E. Wolf in A. J. McKane (ed.), *Scale Invariance, Interfaces, and Non-Equilibrium Dynamics*, 155 ff, Proceedings of NATO Advanced Study Institute, Cambridge, June 1994, Plenum Press, 1994

[8] P. Politi, G. Grenet, A. Marty, A. Pouchet, J. Villain, Phys. Rep. 324 **5-6**, 271, 2000

[9] J. Krug, M. Schimschak, J. Phys. I (France) **5**, 1065, 1995

[10] M. Biehl, M. Kinne, W. Kinzel, S. Schinzer, in: *Proceedings of the 1998 Conference on Computational Physics*, Comp. Phys. Comm. **121 - 122**, 347, 1999

[11] S. Schinzer, M. Kinne, M. Biehl, W. Kinzel, Surface Science **439**, 191, 1999

[12] J. W. Evans, D. E. Sanders, P. A. Thiel, A. E. DePristo, Phys. Rev. B **41** (8), 5410, 1990

[13] J. W. Evans, Phys. Rev. B **43** (5), 3897, 1991

[14] Y. Yue, Y. K. Ho, Z. Y. Dan. Phys. Rev. B **57** (11), 6685, 1998

[15] J. Villain, A. Pimpinelli, L. Tang, D. Wolf, J. Phys. I (France) **2**, 2107, 1992

[16] MPEG videos of our simulations are available online at
`http://theorie.physik.uni-wuerzburg.de/~ahr/LATTICE/lattice.html`

[17] M. Plischke, M. Siegert, J. Krug, Phys. Rev. Lett. **70** (21), 3271, 1993

[18] A.-L. Barabási, H. E. Stanley, *Fractal Concepts in Surface Growth*, Cambridge University Press, Cambridge, 1995

[19] J. Kertész, D. E. Wolf, J. Phys. A: Math. Gen. **21**, 747, 1988

[20] S. Mallat, W. L. Hwang, IEEE Transactions on Information Theory **38**(2), 617, 1992

[21] S. Mallat, S. Zhong, IEEE Transactions on Pattern Analysis and Machine Intelligence, **14**(7), 710, 1992